A green protocol for room temperature synthesis of silver nanoparticles in seconds

Sankar Kalidas Sivaraman, Iniyan Elango, Sanjeev Kumar and Venugopal Santhanam*

Department of Chemical Engineering, Indian Institute of Science, Bangalore 560 012, India

We describe here a rapid, energy-efficient, green and economically scalable room temperature protocol for the synthesis of silver nanoparticles. Tannic acid, a polyphenolic compound derived from plant extracts is used as the reducing agent. Silver nanoparticles of mean size ranging from 3.3 to 22.1 nm were synthesized at room temperature by the addition of silver nitrate to tannic acid solution maintained at an alkaline pH. The mean size was tuned by varying the molar ratio of tannic acid to silver nitrate. We also present proof of concept results demonstrating its suitability for room temperature continuous flow processing.

Keywords: Green synthesis, pH, room temperature, silver nanoparticles, tannic acid.

SIZE- and shape-controlled silver nanoparticles and their assemblies find application in various fields such as plasmonics[1], disease prevention and control[2,3], electronics[4] and catalysis[5]. Commercialization of such applications calls for low-cost production of nanoparticles in bulk quantities that entails continuous flow processing. In this context, rapid, room-temperature and green processes are desirable to minimize capital, design and environmental costs upon scaling up. Presently, redox reaction based batch protocols have emerged as promising avenues for continuous flow processing. However, typical redox synthesis methods use hazardous chemicals as reducing agents or require significant energy input[6]. So, there is a growing interest in the use of environmentally safe 'green' reducing agents. Several recent reports have made significant progress towards this goal by using amino acids, vitamins, polysaccharides and extracts of bio-organisms[7]. Currently, all these green routes utilize reactions that take several minutes to hours to complete at room temperature, and are thus not ideal candidates for bulk production through continuous flow processing. In this communication, we describe a green protocol using tannic acid, a polyphenolic plant extract, as both the reducing and stabilizing agent, and demonstrate its suitability for continuous flow synthesis using a co-axial flow reactor. To the best of our knowledge, this is the first report of a rapid, room temperature protocol for size-controlled metal nanoparticle-synthesis using a green reagent, which is suitable for continuous flow processing.

*For correspondence. (e-mail: venu@chemeng.iisc.ernet.in)

Tannic acid has been studied extensively for its antioxidant properties[8], and as a chelating agent for several inorganic cations[9]. The representative structure of tannic acid, corresponding to its average formula weight, is shown in Figure 1. It consists of a central core of glucose that is linked by ester bonds to polygalloyl ester chains. Tannic acid at its natural acidic pH is known to be a weak reducing agent that can only grow seeds into nanoparticles at room temperature[10]. Tannic acid has a pKa value between seven and eight, depending on its extent of dissociation[11] and is known to partially hydrolyse under mild acidic/basic conditions into glucose and gallic acid units[12]. Gallic acid at alkaline pH reduces silver nitrate into silver nanoparticles rapidly at room temperature[13], but the particles form aggregates in solution as gallic acid is a poor stabilizing agent. Glucose is a weak reducing agent at room temperature, but it is a good stabilizing agent at alkaline pH[14]. These findings suggest that tannic acid could be an ideal reducing and stabilizing agent under alkaline conditions at room temperature.

Prior to use, Teflon® parts and glasswares were cleaned with aqua regia, rinsed with deionized water and dried in a laminar hood. A home built turbine and baffle system, made of Teflon®, designed to fit a 100 ml beaker, was used to provide a standardized mixing environment. Typically, 20 ml of required concentration of aqueous tannic acid (ACS reagent grade, Acros) at pH 8.0 (adjusted by adding K_2CO_3) was taken in the beaker. Then, 5 ml of 2.95 mM silver nitrate (GR grade, Merck) was added as one portion into the tannic acid solution, while stirring. A pale yellow colour appeared almost instantaneously, indicating the formation of silver nanoparticles, and the stirring was continued till there was no perceivable change in colour. The nanoparticles were synthesized over a wide range of values of the initial molar ratio (MR) of tannic

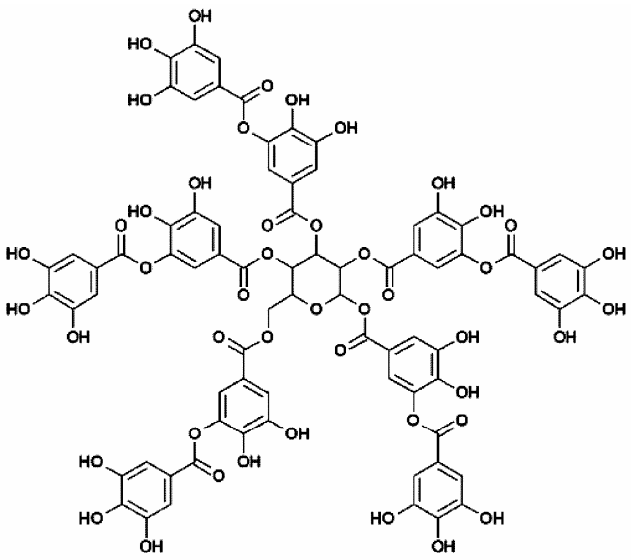

Figure 1. Representative structure of tannic acid ($C_{76}H_{52}O_{46}$).

acid to silver nitrate. Stable colloidal dispersions were formed in all instances.

For continuous flow synthesis, a co-axial flow reactor similar to that described by Hassan *et al.*[15] was fabricated. The inner diameter of the outer tube was 2 mm and that of the inner tube 270 μm. The wall thickness of the inner capillary was 50 μm. A home-built stepper motor controlled syringe was used to dose the reagents. The total volumetric flow rate was 53.97 μl/s and the ratio of the volumetric flow rate of the outer fluid (31.5 μM tannic acid solution at pH 8.0) to that of the inner fluid (2.95 mM silver nitrate solution) was maintained at a value of 12.6 to ensure that the flow pattern was co-axial throughout the length (30 cm) of the microchannel. This avoids particle deposition on the walls of the reactor. The molar flow rates of tannic acid to silver nitrate, averaged over the channel cross-section was maintained at 0.05 for direct comparison with batch synthesis. Figure 2 shows a snapshot of dye flowing through the inner capillary with water as the outer fluid; both fluids having the same volumetric flow rate used for nanoparticle synthesis. This demonstrates the co-axial nature of the flow.

Drop coated samples on carbon film grids or pre-cleaned silicon wafers were imaged using TEM (FEI-Tecnai F30) operated at 200 kV and FESEM (Zeiss-Ultra55) operated at 15 kV respectively. ImageJ[16] software was used to determine the nanoparticle size distribution based on several images from different regions of the sample. UV-Vis spectra were recorded using a double beam spectrometer (Systronics, 2201). pH measurements were made using Orion™ pH electrode and benchtop meter. Stop flow reactor (model SFM/400, Biologic SAS, France) equipped with a diode array spectrophotometer was used to measure the time evolution of absorbance (with 1 ms resolution), after rapidly mixing silver nitrate with tannic acid at the desired molar ratio. The induction time was determined as the time at which there was a detectable change in slope of the absorbance vs time profiles.

Figure 3 *a–c* show representative electron microscopy images (FESEM and TEM) for these samples and the insets represent the part of the UV-Vis spectrum that corresponds to the surface plasmon resonance (SPR) band of silver nanoparticles and the measured particle size distribution of these samples. The mean size is found to depend sensitively on MR. Figure 4 shows the time evolution of absorbance measured using a stop flow module, at the wavelength corresponding to SPR peak for these samples. From Mie theory, the absorbance is directly proportional to volume of nanoparticles (for diameters <20 nm). The

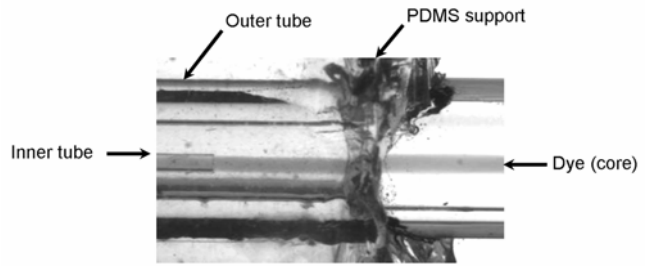

Figure 2. Snapshot of co-axial flow pattern, at various axial locations, visualized using a dye solution as the inner fluid.

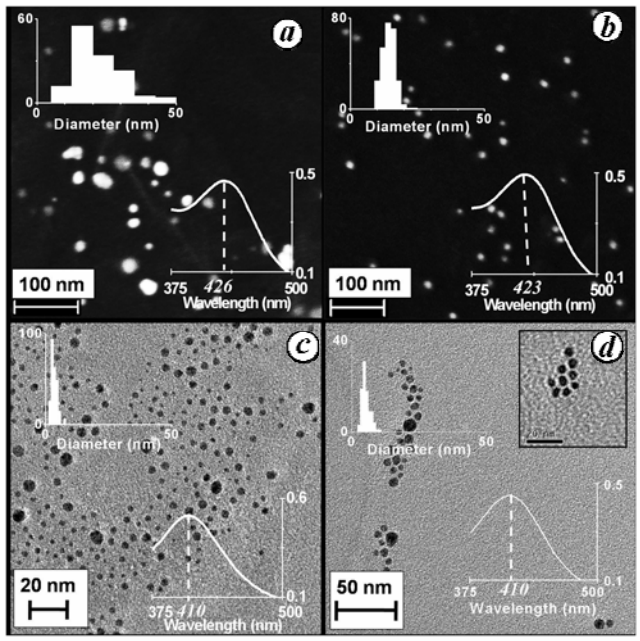

Figure 3. Representative electron microscopy images of silver nanoparticles synthesized at various initial molar ratios (MR) of tannic acid to silver nitrate. (***a***) MR = 1 (FESEM), (***b***) MR = 0.5 (FESEM), (***c***) MR = 0.05 (TEM), (***d***) Silver nanoparticles synthesized in a continuous co-axial flow reactor at molar flow rate ratio of 0.05 (TEM). A magnified image from a different location is also shown at the top right corner (scale bar: 20 nm). The inset graphs in (***a***)–(***d***) depict the corresponding particle size distribution and UV-Vis spectrum, with ordinates representing the actual number of particles counted and absorbance (a.u.) respectively.

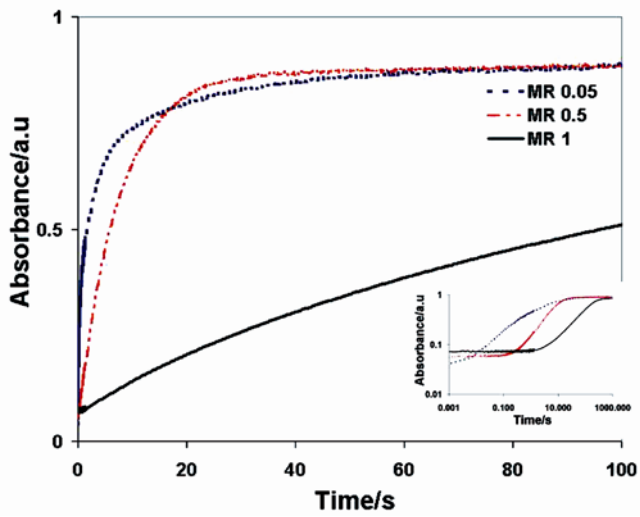

Figure 4. Time evolution of absorbance at SPR peak wavelength for different initial molar ratios (MR) of tannic acid to silver nitrate. The absorbance rises faster for lower MR values. The inset is a logarithmic plot that highlights the variation in induction time.

slope of the absorbance profiles at the early stages is higher for smaller MR values, indicating that the growth rate is higher at smaller MR values. The inset in Figure 4 (logarithmic plot) highlights the variation in induction time, which is the time elapsed between mixing of reactants and formation of detectable particle with MR values. Table 1 summarizes the results of particle size characterization and induction time measurements.

The trends of lower growth rate, and increasing nanoparticle size and induction time with increasing MR is opposite to that expected based on an assumption that increasing reagent concentration should increase reaction rates, thereby resulting in higher monomer concentration leading to faster growth and nucleation. These trends cannot be interpreted in terms of the role of tannic acid as a stabilizer, as increasing stabilizer concentration is also expected to result in smaller sizes. This implies that the role of tannic acid is not limited to that of reducing/stabilizing agent; as, even at alkaline pH, tannic acid has only moderate redox potential[8] and should not nucleate silver nanoparticles at room temperature, just like hydroquinone[17].

To understand these trends and the role of tannic acid in enabling nanoparticle nucleation, it is necessary to elaborate upon the chemistry of tannic acid. Tannic acid has 25 phenolic–OH groups in its structure, but only 10 pairs of *o*-dihydroxyphenyl groups are capable of taking part in redox reactions to form quinones (see Scheme 1) and donate electrons, because of the chelating action of adjacent hydroxyl groups[9,18] and constraints on carbon valency. So, each tannic acid molecule is capable of donating 20 electrons, which implies that an MR value of 0.05 will correspond to stoichiometric requirement. Figure 5 shows UV-Vis spectra of 0.25 ml aliquots sampled during the stepwise addition (corresponding to MR values) of tannic acid solution, maintained at a pH of 8, to 5 ml of 2.95 mM silver nitrate solution. It is seen that the surface plasmon peak of silver nanoparticles at 420 nm increases steadily and then saturates at an MR value of 0.05, indicating that silver nitrate is completely reduced. Also, for MR values ≥ 0.05, a small shoulder at 270 nm is seen that is attributed to the presence of excess tannic acid. The spectrum of a concentrated solution of pure tannic acid at pH 8 is also shown for comparison. These results validate the expected redox stoichiometry of tannic acid and are in agreement with previous results on the chelating capability of tannic acid[19].

Hence, each tannic acid molecule can be thought of as a five-armed chelator[9] and that atomic reorganization occurs within such complexes facilitating nucleation. Thus, at an MR of 0.05, tannic acid complexes will be saturated with 20 silver atoms enabling rapid nucleation (faster induction time) that results in smaller particle size. Whereas at an MR of 1, each tannic acid molecule is on an average ligated to only one silver atom, and so the nucleation rate will be decided by the interaction of such 'unsaturated' compounds in solution leading to slower nucleation rates (larger induction times) that result in larger particle sizes. The role of tannic acid as an organizer during nucleation was first proposed by Chakraborty[20] to model the observed size variation of gold nanoparticles synthesized using Slot and Geuze protocol[21], which could not be explained by homogeneous nucleation models. Turkevich *et al.*[22] also assigned a similar role to acetone dicarboxylic acid in the formation of gold nanoparticles using citrate as the reducing agent. The decrease in initial growth rate with an increase of MR value can also be accounted for by considering that growth occurs due to collision of nuclei/particles with chelated silver atoms. On an average, the rate of collision between chelated silver atoms and nuclei/

Table 1. Variation of induction time for nanoparticle formation and average particle size with the molar ratio of tannic acid to silver nitrate

Molar ratio of tannic acid to silver nitrate (MR)	Induction time (s)	Nanoparticle diameter (nm) ($\mu \pm \sigma$)
0.05	0.008	3.3 ± 1.2
0.5	0.158	14.3 ± 2.1
1	1.52	22.1 ± 5.9

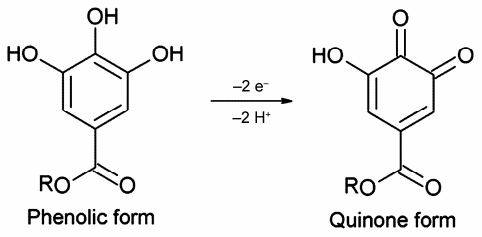

Scheme 1. Oxidation of phenolic group into ketones.

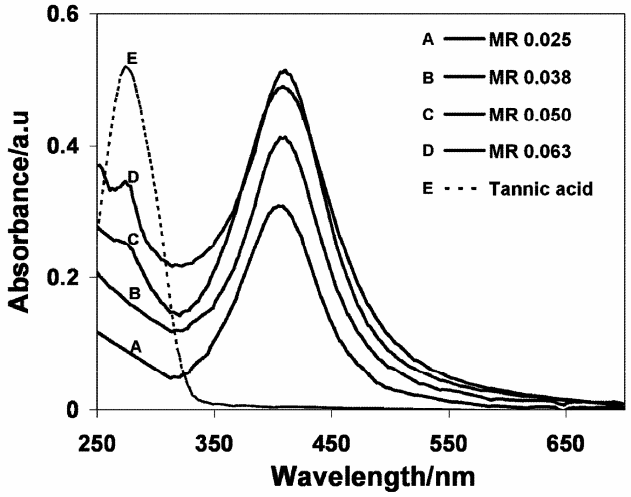

Figure 5. UV-Vis spectra of silver nanoparticle solutions as a function of the initial molar ratio (MR) of tannic acid to silver nitrate. The spectrum of a concentrated (2× original) tannic acid solution is also shown for comparison.

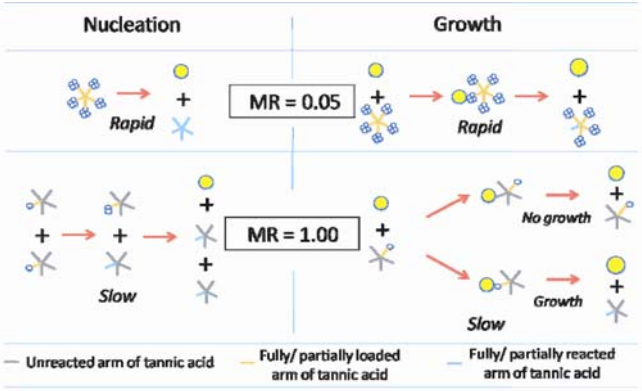

Figure 6. Schematic representation of organizer-based nucleation and growth processes (based on ref. 20) at MR values of 0.05 and 1. Tannic acid is represented as a five armed molecule with each arm capable of reducing and chelating with four silver atoms. Both nucleation and growth processes are faster at MR value of 0.05 as compared to MR value of 1 resulting in the rapid formation of smaller nanoparticles at the lower MR value. Note: the number of loaded atoms depicted is representative of the mean value, given that all the silver ions are reduced and chelated.

particles will be similar in all cases due to opposing effects of increasing concentration and decreasing ligation; however, the probability of incorporation per collision will be higher for compounds ligated with more number of silver atoms. Thus, at smaller MR values, the incorporation efficiency of atoms onto nuclei/particles (i.e. growth) will be higher per collision resulting in higher growth rates. Figure 6 schematically illustrates these concepts at MR values of 0.05 and 1.

Finally, Figure 3 *d* shows the preliminary results of continuous flow synthesis of silver nanoparticles in a co-axial flow microchannel at an MR value of 0.05. The size of the silver nanoparticles was found to be 5.1 ± 1.5 nm. The mean size is higher than the bulk value, whereas the COV is lower. This demonstrates the promise of this protocol for economically scalable continuous flow production of nanoparticles.

In conclusion, tannic acid has been used as a reducing and stabilizing agent to synthesize silver nanoparticles on a timescale of seconds through a simple, green, room temperature protocol, and the suitability of this protocol for energy-efficient, continuous flow synthesis has been demonstrated using a simple co-axial flow reactor. Tannic acid has been previously utilized as a reducing agent in the presence of additional stabilizers[19] or as both the reducing and stabilizing agent[23,24]; but the reaction times reported are 2 h[19] at room temperature and 30 min[23,24] at 80°C, whereas the particle sizes reported are >15 nm. The crucial difference between the present study and the earlier reports is that the pH of the tannic acid solution was adjusted prior to the addition of metal salt. The alkaline pH environment enhanced the reducing and stabilizing capability of tannic acid allowing room temperature synthesis of silver nanoparticles in seconds, and also enabling variation of the mean size from 3 to 22 nm. The increase in particle size with increasing molar ratio of tannic acid to silver nitrate indicates a third role for tannic acid as an organizer for facilitating nucleation. This concept of using tannic acid at alkaline pH as a reducing, organizing, and stabilizing agent is easily extendable to other elements that are known to chelate with tannic acid[9,11].

1. Haes, A. J., Haynes, C. L., McFarland, A. D., Schatz, G. C., Van Duyne, R. P. and Zou, S., Plasmonic materials for surface-enhanced sensing and spectroscopy. *Mater. Res. Bull.*, 2005, **30**, 368–375.
2. Elechiguerra, J. L., Burt, J. L., Morones, J. R., Camacho-Bragado, A., Gao, X., Lara, H. H. and Yacaman, J. M., Interaction of silver nanoparticles with HIV-1. *J. Nanobiotechnol.*, 2005, **3**, doi: 10.1186/1477-3155-3-6.
3. Morones, J. R., Elechiguerra, J.L., Camacho, A., Holt, K., Kouri, J. B., Ramirez, J. T. and Yacaman, M. J., The bactericidal effect of silver nanoparticles. *Nanotechnology*, 2005, **16**, 2346–2353.
4. Markovich, G., Leff, D. V., Chung, S. W., Soyez, H. M., Dunn, B. and Heath, J. R., Parallel fabrication and single-electron charging of devices based on ordered, two-dimensional phases of organically functionalized metal nanocrystals. *Phys. Lett.*, 1997, **70**, 3107–3109.
5. Lewis, L. N., Chemical catalysis by colloids and clusters. *Chem. Rev.*, 1993, **93**, 2693–2730.
6. Cushing, B. L., Kolesnichenko, V. L. and O'Connor, C. J., Recent advances in the liquid-phase syntheses of inorganic nanoparticles. *Chem. Rev.*, 2004, **104**, 3893.
7. Sharma, V. K., Yngard, R. A. and Lin, Y., Silver nanoparticles: green synthesis and their antimicrobial activities. *Adv. Colloid Interface Sci.*, 2009, **145**, 83–96.
8. Hagerman, A. E., Riedl, K. M., Jones, G. A., Sovik, K. N., Ritchard, N. T., Hartzfeld, P. W. and Riechel, T. L., High molecular weight plant polyphenolics (tannins) as biological antioxidants. *J. Agric. Food Chem.*, 1998, **46**, 1887–1892.
9. McDonald, M., Mila, I. and Scalbert, A., Precipitation of metal ions by plant polyphenols: optimal conditions and origin of precipitation. *J. Agric. Food Chem.*, 1996, **44**, 599–606.
10. Tian, X., Wang, W. and Cao, G., A facile aqueous-phase route for the synthesis of silver nanoplates. *Mater. Lett.*, 2007, **61**, 130–133.
11. Cruz, B. H., Diaz-Cruz, J. M., Arino, C. and Esteban, M., Heavy metal binding by tannic acid: a voltammetric study. *Electroanalysis*, 2000, **12**, 1130–1137.
12. Bors, W., Foo, L. Y., Hertkorn, N., Michel, C. and Stettmaier, K., Chemical studies of proanthocyanidins and hydrolyzable tannins. *Antioxid. Redox Signal.*, 2001, **3**, 995–1008.
13. Martinez-Castanon, G. A., Nino-Martinez, N., Martinez-Gutierrez, F., Martinez-Mendoza, J. R. and Ruiz, F., Synthesis and antibacterial activity of silver nanoparticles with different sizes. *J. Nanopart. Res.*, 2008, **10**, 1343–1348.
14. Liu, J., Qin, G., Raveendran, P. and Ikushima, Y., A facile and green synthesis, characterization, and catalytic function of b-D-glucose stabilized Au nanocrystals. *Chem. Eur. J.*, 2006, **12**, 2131–2138.
15. Hassan, A. A., Sandre, O., Cabuil, V. and Tabeling, P., Synthesis of iron oxide nanoparticles in a microfluidic device: preliminary results in a co-axial flow millichannel. *Chem. Commun.*, 2008, 1783–1785.
16. Rasband, W. S., 1997–2008; http://rsb.info.nih.gov/ij/
17. Gentry, S. T., Fredericks, S. J. and Krchnavek, R., Controlled particle growth of silver sols through the use of hydroquinone as a selective reducing agent. *Langmuir*, 2009, **25**, 2613–2621.
18. Yoosaf, K., Ipe, B. I., Suresh, C. and Thomas, K. G., *In situ* synthesis of metal nanoparticles and selective naked-eye detection of

lead ions from aqueous media. *J. Phys. Chem. C*, 2007, **111**, 12839–12847.
19. Sun, L., Zhang, Z. J., Wu, Z. S. and Dang, H. X., Synthesis and characterization of DDP coated Ag nanoparticles. *Mater. Sci. Eng. A*, 2004, **379**, 378–383.
20. Chakraborty, J., Modelling and simulation frameworks for synthesis of nanoparticles. Ph D thesis, IISc, 2009.
21. Slot, J. W. and Geuze, H. J., A new method of preparing gold probes for multiple-labeling cytochemistry. *Eur. J. Cell Biol.*, 1985, **38**, 87–93.
22. Turkevich, J., Stevenson, P. C. and Hillier, J., A study of the nucleation and growth processes in the synthesis of colloidal gold. *Discuss. Faraday Soc.*, 1951, **11**, 55–75.
23. Zhao, S. Y., Chen, S. H., Li, D. G., Yang, X. G. and Ma, H. Y., A convenient phase transfer route for Ag nanoparticles. *Physica E*, 2004, **23**, 92–96.
24. Bulut, E. and Oezacar, M., Rapid facile synthesis of silver nanoparticles using hydrolysable tannins. *Ind. Eng. Chem. Res.*, 2009, **48**, 5686–5690.

ACKNOWLEDGEMENTS. We thank DST, New Delhi and the IISc Centre for Excellence in Nanoelectronics for funding. INI Centre at IISc is acknowledged for TEM facilities.

Received 17 July 2009; accepted 21 August 2009

Adsorption of non-petroleum base surfactant on reservoir rock

Subrata Borgohain Gogoi

Department of Petroleum Technology, Dibrugarh University, Dibrugarh 786 004, India

Surfactant loss due to adsorption on the reservoir rock is one of the major concerns in enhanced oil recovery (EOR) processes. It weakens the effectiveness of the injected slug in reducing oil–water interfacial tension (IFT) and makes the process uneconomical. In this study, an attempt is made to investigate the adsorption of Na-lignosulphonate onto the porous media of Oil India Limited (OIL) petroleum reservoir rocks. The data were interpreted from the well-known models and it was found that the Langmuir model is a good fit for the pH and brine data over the entire range of variables. Adsorption increases with NaCl concentration and decreases with increase in pH.

Keywords: Adsorption, brine, Na-lignosulphonate, pH, reservoir rock.

SURFACTANT molecules adsorb well to solid interfaces such as the porous media found in petroleum reservoirs. The adsorbed surfactant layer represents both an additional resistance to flow as well as loss of surfactant properties and is therefore, of fundamental importance in the enhanced oil recovery (EOR) process that involves the flow of surfactant solution through porous media.

e-mail: sbg6@rediffmail.com

According to Austad and Milter[1], chemical flooding of oil reservoirs is one of the most successful methods to enhance oil recovery from depleted reservoirs at low pressure. However, on a volume basis, the greatest potential usage would be surfactant flooding for EOR[2]. The 1970s and 1980s were active periods for research on surfactants for EOR and a large number of patents were issued.

Surfactant adsorption in the flow of surfactant solutions through porous media is usually accompanied by a variety of additional complex phenomena. Viscoelasticity has contributed to the increase in flow resistance, particularly at high-flow velocities[3–6]. Consequently, the effect of adsorption on permeability reduction was often not clear. In addition, phenomena such as mechanical entrapment and hydrodynamically induced retention obscure the role adsorption plays in surfactant retention and mobility reduction[7–12]. Much effort has been devoted to qualify the contribution of surfactant adsorption to mobility reduction and surfactant retention in both consolidated and unconsolidated porous media. The existing studies, however, do not quantify the resistance of the adsorbed surfactant layer to the flow of surfactant solutions.

Success or failure of a surfactant flood may depend on the degree of retention of surfactants during EOR operation and one of the possible mechanisms of the surfactant retention was the solid–liquid interface. Several papers dealing with the adsorption of commercially available surfactants have been published[13–18], but meaningful comparison of reported data was quite difficult because surfactants of various degrees of purity have been used.

Zaitoun *et al.*[19] conducted a series of experiments on surfactant screening and evaluation for surfactant flooding in the Chihuido de la Sierra Negra field in Argentina. They developed a new anionic surfactant that provides good solubility in high salinities and low interfacial tension at low concentrations. Gogoi[20] described that sodium lignosulphonate formed as a waste in paper industries had the potential to be used in EOR.

Adsorption minimizes the loss of the high equivalent weight fraction that was most efficient in lowering the interfacial tension (IFT)[21]. Adsorption of surfactants considered for EOR applications have been studied extensively over the last few years[22–27] and it has convincingly shown that it is possible to develop surfactant systems which displace oil from porous media almost completely when used in large quantities. Effective oil recovery by surfactant was not a question of technical feasibility but rather a question of economics. Clays in the rock have high surface area that can affect the surfactant flood in many ways. Bernard[28] has suggested that by ion-exchange, divalent ions were transferred to the surfactant solution from the clays resulting in precipitation of surfactant and loss of surfactant in the displacing fluid. It was found that for a particular sulphonate, the minimum tension between a salt solution containing the sul-